

THE STUDY OF THE LOWER IONOSPHERE AT LOW LATITUDE

Thesis

Presented by

S.P.GUPTA

to the

Gujarat University Ahmedabad

for the Ph.D. degree.

043



B3717

Physical Research Laboratory

Ahmedabad - 9.

January 1970

## STATEMENT

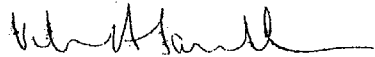
The work presented in this thesis is based on the results obtained from the rocket borne Langmuir probe and plasma noise probe studies over Thumba near geomagnetic equator. Working under the guidance of Prof.V.A.Sarabhai and Prof.Satya Prakash at the Physical Research Laboratory, the author was responsible for the design and development of the plasma noise probe that was employed to study the fluctuations in Langmuir probe current which is termed as plasma noise in the thesis. The necessary telemetry system which includes subcarrier oscillators and band pass filters as per I.R.I.G. specifications was developed by the author. A spectrum analyser was also developed to study the spectrum of the observed plasma noise. The author also made improvements in the Langmuir probe system.

The author took active part in extensive testing and checking of the Langmuir probe and plasma noise probe system prior to launching. He was also responsible for analysing the data and interpreting the experimental results.

The Langmuir probe was employed to determine the electron density and electron temperature while the plasma noise probe was used to study the Langmuir probe current fluctuations with amplitudes as low as 0.05% in the frequency range 70 Hz to 1 KHz. Fluctuations with frequencies less than 70 Hz can be studied directly from the telemetry record of the Langmuir probe current. These measurements of ionospheric irregularities have been interpreted in terms of processes taking place in the equatorial

ionosphere. Many conclusive results have come out from the present study.

The results presented in the thesis contain probably the first in situ measurements of equatorial E region irregularities with scale sizes of the order of a few meters. They also contain probably the first systematic in-situ measurements of disturbances created in the medium by a moving rocket. It is believed that ion acoustic waves are generated in the wake of a vehicle moving through the ionosphere, but so far no in-situ measurements were available. The present results therefore provide fresh insights into plasma instabilities in the equatorial ionosphere and the disturbances produced by the rocket.

  
Prof. V.A. Sarabhai  
Director  
Physical Research Laboratory  
Navrangpura  
Ahmedabad-9

S. P. Gupta  
S. P. Gupta  
Author

January 24, 1970

## ACKNOWLEDGEMENT

The author is indebted deeply to Professor Satya Prakash for the guidance, supervision and encouragement, he gave throughout the period of the work. Prof.V.A.Sarabhai took keen interest in guidance and gave valuable advice for which author expresses sincere gratitude to him.

It is a great privilege to thank Prof.K.R.Ramanathan and Prof.F.R.Pisharoty for valuable discussions and suggestions. Thanks are due to Dr.B.H.Subbaraya for going through the manuscript of the thesis and suggesting many improvements.

Sincere thanks are expressed to Mr.H.G.S. Murthy, Director, Thumba Equatorial Rocket Launching Station and his colleagues Messrs A.P.J.Abdul Kalam, R.Aravamudan, D.Easwardas, P.P.Kale, B.Ramakrishna Rao and G.Madhavan Nair whose enthusiastic cooperation made rocket launchings successful. The author is also thankful to Dr.B.V.Krishnamurthy for providing ionograms.

Acknowledgements are also due to National Aeronautics and Space Administration, U.S.A. for supplying the Nike-Apache rockets. Thanks are also due to Atomic Energy Commission, Government of India and Indian National Committee for Space Research for financial assistance. The author is very grateful to Ministry of Education, Government of India for the award of a scholarship.

It is a particular pleasure to express gratitude to Messrs N.S. Savalgi for preparing payload circuitry, R.I. Patel for his help in data analysis, and C.L.Gajjar for making mechanical parts of the payload.

*S.P. Gupta*  
S.P. GUPTA.

## LIST OF CONTENTS

### Chapter I

#### Introduction

1.1	The equatorial D region.	2
1.2	The equatorial E region.	3
1.3	The equatorial electrojet.	4
1.4	Electric field in the equatorial E region.	6
1.5	Equatorial electrojet irregularities.	7
1.6	Necessity of the present study.	8

### Chapter II

#### Production Mechanisms of equatorial electrojet irregularities.

2.1	The cross-field instability.	19
2.2	The two stream instability.	21
2.3	Plasma turbulence.	24

### Chapter III

#### Experimental techniques. Theory of Langmuir probe and Plasma noise probe.

3.1	Ground based techniques.	30
3.2	Rocket and satellite borne techniques.	32
3.3	Langmuir probes used for ionospheric studies.	33
3.4	Theory of Langmuir probe.	34
3.5	Electron temperature from first derivative of Langmuir probe characteristic.	40

3.6	Langmuir probe for ionospheric studies.	41
3.7	Small scale irregularities measurement by Plasma noise probe.	45
3.8	Theory of Plasma noise probe.	46
3.9	Sampling of irregularities by moving rocket.	47
3.10	Environmental conditions around the moving rocket.	51
3.11	Production of disturbances in Plasma by moving rocket.	53

#### Chapter IV

##### Instrumentation

4.1	The conventional Langmuir Probe system.	55
4.2	The present system.	57
4.3	Description of the Langmuir Probe and Plasma noise probe.	59
4.4	Electrode Geometry.	60
4.5	Probe electronics.	61
4.6	Sweep circuit.	62
4.7	Electrometer amplifier.	65
4.8	Plasma noise amplifier.	70
4.9	Electronic differentiation of Langmuir Probe characteristic.	72
4.10	Subcarrier Oscillator.	72
4.11	Power supply.	75
4.12	Spectrum analyser.	76
4.13	Wiring of the payload circuits.	76
4.14	Dotting of the payload.	77
4.15	Telemetry requirements.	78

4.16	Mounting and fixing of the payload and probe.	80
4.17	Pre-launch testing.	81

## Chapter V

### Experimental results

Summary of Langmuir Probe and Plasma noise probe flights.

5.1	Nike - Apache 10.11	85
5.2	Nike - Apache 10.13	91
5.3	Nike - Apache 20.07	96
5.4	Nike - Apache 20.08	97

## Chapter VI

### Discussion of experimental results.

6.1	Ionisation irregularities	100
6.2	Summary of the results	108
6.3	Discussion	110
6.4	Irregularities due to rocket motion.	123
6.5	Equatorial D region electron density.	127
6.6	The equatorial E-region during afternoon hours.	129
6.7	The equatorial E region during evening twilight.	129
6.8	The E region over Thumba around mid-night	131
6.9	Electron temperature in the equatorial E region.	134



Chapter VII

Summary and conclusions

138

References

i to viii

## List of Figures

		<u>Page</u>
Figure 1	Simplified picture of one mode of operation of the instability.	20 (a)
Figure 2	Typical Langmuir Probe characteristic.	36 (a)
Figure 3	Schematic representation of the sampling process of irregularities by moving rocket. Lines indicate the irregularity wave fronts while arrow indicates the rocket.	48
Figure 4	Schematic representation of the disturbed regions in the vicinity of the moving bodies of various shapes From Alpert 1965)	53 (a)
Figure 5	Contact Potential versus time after launch for day and night flights.	53 (b)
Figure 6	Rocket borne Langmuir Probe system (a) Conventional system (b) Present system.	56 (a)
Figure 7	Functional diagram of the Langmuir and Plasma noise probe system.	58 (a)
Figure 8	Nose tip electrode photograph.	61 (a)
Figure 9	Block diagram of sweep generator.	62
Figure 10	Circuit diagram of sweep generator.	63 (a)
Figure 11	Various wave forms at different terminals of the sweep circuit.	64 (a)
Figure 12	Block diagram of 100% current feedback amplifier.	66
Figure 13	Electrometer amplifier circuit.	67 (a)
Figure 14	Zero marker and resistance to Thyrite switching circuit.	68 (a)
Figure 15	Calibration curves of electrometer amplifier	70 (a)

Figure 16	Plasma noise probe amplifier circuit.	70 (b)
Figure 17	Phase inverter and detector circuit.	71 (a)
Figure 18	Subcarrier Oscillator circuit.	73 (a)
Figure 19	Input voltage versus frequency curve of Subcarrier Oscillator	74 (a)
Figure 20	Characteristic curve of band-pass filter.	
Figure 21	Voltage regulator circuit.	75 (b)
Figure 22	Plasma noise probe data recording system using spectrum analyser.	76 (a)
Figure 23	Response curve of spectrum analyser.	76 (b)
Figure 24	Photograph of wired circuit.	77 (a)
Figure 25	Photograph of Langmuir probe and Plasma noise probe layload.	77 (b)
Figure 26	Installation of Langmuir Probe, Plasma noise probe and Telemetry system in a Nike-Apache rocket.	80 (a)
Figure 27	Integrated payload block diagram.	81 (a)
Figure 28	Control box for monitoring the payload from block house.	81 (b)
Figure 29	Sketch diagram of nose tip electrode.	85 (a)
Figure 30	Electron density profile for evening flight 10.11.	89 (a)
Figure 31	A semilog plot of electron current versus probe voltage.	89 (b)
Figure 32	Electron temperature for evening flight 10.11.	89 (c)
Figure 33	Percentage fluctuations in probe current for evening flight 10.11.	91 (a)

Figure 34	Electron density profile for evening flight 10.13.	94 (a)
Figure 35	Percentage fluctuations in probe current in frequency range 70 Hz to 1 KHz.	95 (a)
Figure 36	Amplitude of irregularities in various scale sizes in arbitrary units.	95 (b)
Figure 37	Typical curve for log - log plot of percentage amplitude and frequency for Plasma noise.	96 (a)
Figure 38	Spectral index values for flight 10.13.	96 (b)
Figure 39	Electron density profile for mid-day flight 20.07.	97 (a)
Figure 40	Electron temperature for mid-day flight 20.07.	97 (b)
Figure 41	Percentage fluctuations in probe current in frequency range 70 Hz to 1 KHz for mid-day flight 20.07.	98 (a)
Figure 42	Electron density profile for mid-night flight 20.08.	98 (b)
Figure 43	Electron temperature for mid-day night flight 20.08.	98 (c)
Figure 44 a)	Percentage fluctuations in (30-300 meters scale size,) probe current and electron density, (ascent) profile for flight 20.08.	99 (a <sub>1</sub> )
b)	Percentage fluctuations in (30-300 meters scale size) probe current and electron density, (descent) profile for flight 20.08.	99 (a <sub>2</sub> )
Figure 45	Percentage fluctuations in probe current in frequency range 70 Hz to 1 KHz for flight 20.08.	99 (b)
Figure 46	Spectral index values for flight 20.08.	99 (c)

Figure 47 (a)	Telemetry record obtained at 87 Km.	103 (a)
Figure 47 (b)	Telemetry record obtained at 96 Km.	104 (a)
Figure 47 (c)	Telemetry record obtained at 171 Km.	104 (b)
Figure 48 (a)	Spectrum analyser output record at 87 Km.	105 (a)
Figure 48 (b)	Spectrum analyser output record at 96 Km.	105 (b)
Figure 48 (c)	Spectrum analyser output record at 171 Km.	124 (a)

---